TUNING SPECTRAL AND TEMPORAL RESPONSE OF UV-PUMPED COLLOIDAL QUANTUM DOTS DISPERSED WITHIN ADDITIVELY-MANUFACTURED STRUCTURES

1st Lt Michael Sherburne, Dr. Sergei Ivanov, Ms. Shruti Gharde, Ms. Gema Alas, Mr. Arjun Senthil, Mr. Dominic Bosomtwi, Dr. Nathan Withers, Dr. Marek Osiński, Dr. Larry Burggraf, Dr. Thomas Weber, Maj Tod Laurvick, PhD

25 January 2021

Technical Memorandum

AIR FORCE INSTITUTE OF TECHNOLOGY
Graduate School of Engineering and Management (AFIT/EN)
2950 Hobson Way
AIR FORCE EDUCATION TRAINING COMMAND
WPAFB, OH 45433-7765

NOTICE AND SIGNATURE PAGE

Using Government drawings, specifications, or other data included in this document for any purpose other than Government procurement does not in any way obligate the U.S. Government. The fact that the Government formulated or supplied the drawings, specifications, or other data, does not license the holder or any other person or corporation; or convey any rights or permission to manufacture, use, or sell any patented invention that may relate to them.

Qualified requestors may obtain copies of this report from the Defense Technical Information Center (DTIC) (`http://www.dtic.mil`).

AFIT-22-ENG01007 HAS BEEN REVIEWED AND IS APPROVED FOR PUBLICATION IN ACCORDANCE WITH ASSIGNED DISTRIBUTION STATEMENT.

SHERBURNE.MICHAEL.D.1050457466 Digitally signed by SHERBURNE.MICHAEL.D.1050457466 Date: 2022.01.25 12:55:39 -07'00'

1ST LT MICHAEL SHERBURNE
Graduate Student
Department of Electrical and Computer Engineering

CHANDRAHALIM.HENGKY.1540631324 Digitally signed by CHANDRAHALIM.HENGKY.1540631324 Date: 2022.01.25 16:34:36 -05'00'

DR. HENGKY CHANDRAHALIM
Assistant Professor
AFIT/ENG

This report is published in the interest of scientific and technical information exchange, and its publication does not constitute the Government's approval or disapproval of its ideas or findings.

REPORT DOCUMENTATION PAGE

Form Approved

OMB No. 0704-0188

1. REPORT DATE *(DD-MM-YYYY)*
25-01-2022

2. REPORT TYPE
Technical Memorandum

3. DATES COVERED *(From - To)*
07-25-2018 to 12-9-2021

4. TITLE AND SUBTITLE
Tuning Spectral and Temporal Response of UV-pumped Colloidal Quantum Dots Dispersed Within Additively-Manufactured Structures

5a. CONTRACT NUMBER

5b. GRANT NUMBER
NA000103, 89233218CNA000001, N00014-17-1-2975,N00014-19-1-2117, N00014-18-1-2739

5c. PROGRAM ELEMENT NUMBER

6. AUTHOR(S)
Michael Sherburne* Sergei Ivanov** Shruti Gharde*** Gema Alas*** Arjun Senthil*** Dominic Bosomtwi*** Nathan Withers*** Marek Osiński*** Larry Burggraf* Los Alamos National Laboratory Thomas Weber**** Tod Laurvick*

5d. PROJECT NUMBER

5e. TASK NUMBER

5f. WORK UNIT NUMBER

7. PERFORMING ORGANIZATION NAME(S) AND ADDRESS(ES)
Air Force Institute of Technology*
Graduate School of Engineering and Management (AFIT/EN)
2950 Hobson Way
WPAFB, OH 45433-7765

Center for Integrated Nanotechnologies**
P.O. Box 5800, MS-1315
Albuquerque, NM 87185-1315

UNM Center for High Technology Materials***
1313 Goddard SE, MSC04 2710
Albuquerque, NM 87106-4343

Los Alamos National Laboratory****
PO Box 1663, Mail Stop E526
Los Alamos, NM 87545

8. PERFORMING ORGANIZATION REPORT NUMBER
AFIT-22-ENG01007

9. SPONSORING/MONITORING AGENCY NAME(S) AND ADDRESS(ES)
National Nuclear Security Administration
U.S. Department of Energy
1000 Independence Ave., SW
Washington, DC 20585

Office of Naval Research
875 N. Randolph Street
Suite 1425
Arlington, VA, 22203

10. SPONSOR/MONITOR'S ACRONYM(S)
NNSA, ONR

11. SPONSOR/MONITOR'S REPORT NUMBER(S)

12. DISTRIBUTION/AVAILABILITY STATEMENT
Distribution statement A approved for public release; distribution is unlimited. Public Affairs release approval 88ABW-2022-0038. Other requests for this document shall be referred to AFIT/EN, 2950 Hobson Way, WPAFB, OH 45433-7765.

13. SUPPLEMENTARY NOTES

14. ABSTRACT
Additive manufacturing is opening up new ways to make structures. Consequently, there are a growing areas of research in using additive manufacturing with nanomaterials. This paper investigates a novel fabrication technique which utilizes 3D printed honeycomb structures loaded with colloidal quantum dots through external dispersion and capped with SU-8-5 photoresist. Both the thickness of the 3D printed structure and the volume of colloidal quantum dots loaded into the aforementioned 3D printed structures affects both the photoluminescence spectra and photoluminescence lifetime decay of the overall sample. A charge transfer peak at ≈ 460 nm is observed in this process, which exhibits photoluminescence intensity tunability. It has been found that both the relative photoluminescence intensity at the charge transfer peak (0.197 to 0.874) and the photoluminescence lifetime decay at the colloidal quantum dots' main peak of emission (15.5 ns-77.7 ns) are tunable by tweaking the fabrication process. These findings pave the way for future optimization of this technique for sensing applications.

15. SUBJECT TERMS
additive manufacturing; characterization; nanotechnology; photoluminescence decay; photoluminescence spectra; quantum dots; temporal response

16. SECURITY CLASSIFICATION OF:			**17. LIMITATION OF ABSTRACT**	**18. NUMBER OF PAGES**	**19a. NAME OF RESPONSIBLE PERSON**
a. REPORT	**b. ABSTRACT**	**c. THIS PAGE**			1st Lt Michael Sherburne
UNCLASSIFIED	UNCLASSIFIED	UNCLASSIFIED	SAR	14	**19b. TELEPHONE NUMBER** *(include area code)* 505-846-6659, research@afit.edu

Standard Form 298 (Rev. 8-98)
Prescribed by ANSI Std. 239.18

TABLE OF CONTENTS

Section **Page**

LIST OF FIGURES

Figure **Page**

1.0 INTRODUCTION

Optical sensors are useful for a wide variety of industries, ranging anywhere from cameras used on one's mobile phone, Night Vision Goggles (NVG)s for pilots, and streak cameras to measure fast photons. When it comes to the need for measuring fast optical events in the picoseconds to nanoseconds range, nanomaterials can be used. Well established nanomaterials called Colloidal Quantum Dot (CQD)s can be affordably bought as Commercially-Off-The-Shelf (COTS) products. CQDs can be used in various types of sensing applications such as: radiation, temperature, electromagnetics, strain, up-converting of wavelengths when paired with another material, and many more [1].

In order to use CQDs as sensors, one can utilize them in their liquid form, impregnate them within a polymer matrix, disperse as a thin-film layer, or drawn within a Photonic Crystal Fiber (PCF) [1]. Recently, the application of CQDs can be done by using them within extrusion material of 3D printers [2, 3]. However, CQDs dispersed into 3D printed parts after the 3D structure's fabrication using conventional 3D printing technology has not been characterized yet. There is an interesting question regarding if both the CQDs' Photoluminescence (PL) intensity and PL lifetime decay can be tuned by changing the structural fabrication process. This would allow one to change the optical emission of their sensor in an affordable manner by using the same nanomaterials.

Taking inspiration from drawing up CQDs within a PCF, this paper investigated dispersing CQDs into a honeycomb 3D printed structure. Design of Experiments (DoE) was used in order to determine if both the PL intensity and PL lifetime decay can be optimized by varying both the volume of dispersed CQDs into the 3D printed structure and the thickness of the 3D printed structure itself [1].

2.0 THEORY

Every CQD contains a core, the primary compound [4]. In order to both prevent agglomeration of the nanocrystals and ensure compatibility of the nanocrystals into various media, ligands are bonded to the CQD's surface. Ligands are organic polymer chains that help to functionalize the CQDs [5]. During synthesis of CQDs, defects occur across the surface of the core. To mitigate this issue, a shell compound material (usually ZnS) is applied around the core. The shell fills in core defects and reduces trap states, thus increasing Quantum Efficiency (QE) [6]. In addition, shells usually promote a Stokes shift (separation of the emission and absorption spectra) [6, 7]. This also helps increase QE as reabsorption of emitted photons may be greatly mitigated or even eliminated [8].

The energy transitions within CQDs have discrete energy levels near the band edges. They are confined in a small three dimensional structure whose width of confinement (e.g, spherical CQD diameter) will determine the bandgap energy between the Highest Occupied Molecular Orbital (HOMO) and Lowest Unoccupied Molecular Orbital (LUMO)

levels. The HOMO is the highest occupied discrete energy state above the valence band edge and the LUMO is the lowest unoccupied discrete energy state below the conduction band edge. In addition, an excited electron promoted from the valence band to the conduction band will leave a hole and form an exciton (an electron-hole pair that is kept together by Coulomb interaction) [9, 10]. Photon emission of a CQD occurs when an exciton relaxes back to its ground state (valence band) [9].

3.0 APPARATUS AND METHODS

Two nanomaterials (supplied by NN-Labs) were used due to a need for more CQDs in order to create all the samples needed to perform the design of this experiment. They were bought as a 10 mg by weight colloidal solutions in toluene. The materials used were: CdSe/ZnS (520 nm emission) and InP/ZnS (530 nm emission). The reason why their emission wavelengths were different by 10 nm was because the two CQD materials were not sold as both 520 nm or 530 nm. These CQDs were then dispersed into honeycomb 3D printed structures with $500\,\mu m$ diameter holes glued onto a thin $2.4892\,cm$ diameter quartz disc. The structures were fabricated by using a VisiJet M3 Navy ProJet MJP 3600 Series printer using the UHD setting.

The samples for the design of this experiment used the following three levels for factor one (volume of CQDs loaded into structure): $40\,\mu L$, $80\,\mu L$, and $160\,\mu L$. The three levels for factor two (thickness of structure) were: $240\,\mu m$, $480\,\mu m$, and $960\,\mu m$. CdSe/ZnS CQDs were used for the following pairs of factor one and factor two respectively: 40/240, 40/960, 80/480, 80/960, and 160/960. InP/ZnS were used for the following pairs of factor one and factor two respectively: 40/480, 80/240, 160/240, and 160/480. Due to limited resources, only one replication of the fabricated structures were possible at the time of this study.

The following recipe was used to fabric each sample used in the design of this experiment: print out 3D printed structure; heat structure in hot oven at 70℃ for 30 minutes on top of a perforated aluminum sheet to remove wax; use boiling water (250℃) to remove remaining supporting wax in 3D print; use pressurized nitrogen gas to dry off the 3D print, submerge 3D print back into boiling water, then quickly drop into a glass jar filled with water to keep it hydrophilic. Once ready to add nanocrystals: drop Isopropyl Alcohol (IPA) onto top of honeycomb structure; disperse CQDs using a micropipette to top of structure; let dry for five minutes; place honeycomb structure on top and center of quartz disc; apply SU-8-5 around circumference of 3D printed honeycomb structure; Ultra Violet (UV) cure for 1000 s; apply SU-8-5 to top of honeycomb structure on top of a spin coater; after UV curing edges, ramp-up speed: 500 RPM, spin speed: 3000 RPM; UV cure for 1000 s; remove excess photoresist on back of quartz disc using acetone, IPA, then water; and finally nitrogen blow dry the sample.

Drawings and pictures of the 3D printed honeycomb structure can be read in Ref. [1]. After fabrication, each sample was first tested for its PL spectra and then its PL lifetime decay.

3.1 PL Spectra Measurement Setup

Measurements were conducted at approximately room temperature (23℃). A PL spectrofluorometer system (Horiba-Jovin Fluorolog-3) was used and the following settings were: rotation of sample holder (right-angle), sample holder angle ($30°$), integration time (0.1 s), wavelength increment (1.00 nm), side entrance slit (1.00 nm), front exit slit (1.00 nm), grating was set to density 1200 $\frac{\text{grooves}}{\text{mm}}$ (Blaze: 500 nm), and averaged scans was set to five. Excitation wavelengths for each nanomaterial were the following: CdSe/ZnS (395 nm), InP/ZnS (405 nm), and control (275 nm). All PL intensities collected for the PL spectra experiment were normalized due to the differences in photon counts between different CQDs and the intensity of the excitation lamp was not constant throughout the entire excitation range of the PL spectrometer. QE data was not collected due to issues with the hardware. However, these limitations of this study were of no issue as the intent of this paper was to look at both relative changes of Charge Transfer (CT) and PL lifetime decay.

3.2 UV-Vis PL Lifetime Decay Setup

The UV-Vis PL lifetime decay was conducted at Center for Integrated Nanotechnologies (CINT) within Sandia National Laboratory (SNL). The equipment used was the PTI Felix 32 Spectrofluorimeter and the software used was FeliX Analysis module version 1.2. The available PL decay temporal resolution was ≈ 500 ps. This comes from the Guassian shape from the excitation diodes that had an $\approx 1.2 - 1.4$ ns Full Width at Half Maximum (FWHM) and the decay measurement began once the excitation source decayed, hence the temporal resolution was about half of the FWHM of the excitation diode pulse. An excitation wavelength of 405 nm was selected. The software used considered the Instrument Response Function (IRF) when calculating the multicomponent exponential fitting values. The following settings were used for each PL decay spectra: decay was averaged (3x), integration time (0.5 s), and the number of data points (100). The peak emission of each CQD material (520 nm and 530 nm) was measured. All PL intensities were normalized due to the inherent differences (albeit, a difference of $\approx 10\%$ between counts per second during a comparison test) in QE between the different CQD materials. The multicomponent exponential fitting model was used and represented by equation 1.

$$F(t) = F_0 + A_1 \ \exp -\frac{t - t_0}{\tau_1} + A_2 \ \exp -\frac{t - t_0}{\tau_2} + ... \tag{1}$$

From equation 1, F_0 is the initial intensity, $A_{\#\text{s}}$ are the preexponential components, $\tau_{\#\text{s}}$ are the decay constants in ns, t is present time in ns, and t_0 is the initial time in ns. The multicomponent exponential model using anywhere from two to four exponential

components is similar to the bi-exponential model which has been determined to make a good approximated fit of a CQD's decay [11].

4.0 RESULTS AND DISCUSSIONS

First, this section goes over the PL spectra tunability when changing both the thickness of the 3D printed structure and the volume of CQDs loaded into the structure. PL spectra collected for all samples can be seen in Fig. 1.

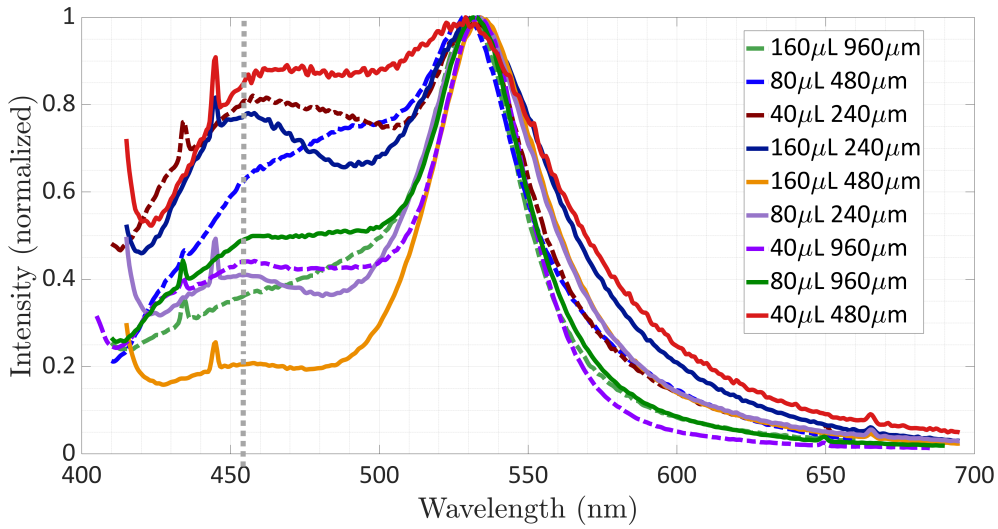

Figure 1. PL spectras showing both CQDs' main peak of emission and CT peak of emission at ≈ 460 nm (located on gray dashed vertical line).

The secondary peak that appeared at ≈ 460 nm was due to CT from the CQDs transferring to the surrounding SU-8-5 polymer material used as a capping material [12–14]. It was determined not to be Förster Resonance Energy Transfer (FRET) due to the CT peak occurring at a higher energy wavelength (a blue shift) [15]. The control sample emitted a peak wavelength at 365 nm whose spectra can be seen in Ref. [1]. Thus, this new CT peak only occurred once CQDs were loaded into the structure. Minitab was utilized to create a contour plot at the 460 nm peak. This plot is seen in Fig. 2. For the raw data entered into Minitab, the reader is encouraged to read the table in Appendix W. of Ref. [1].

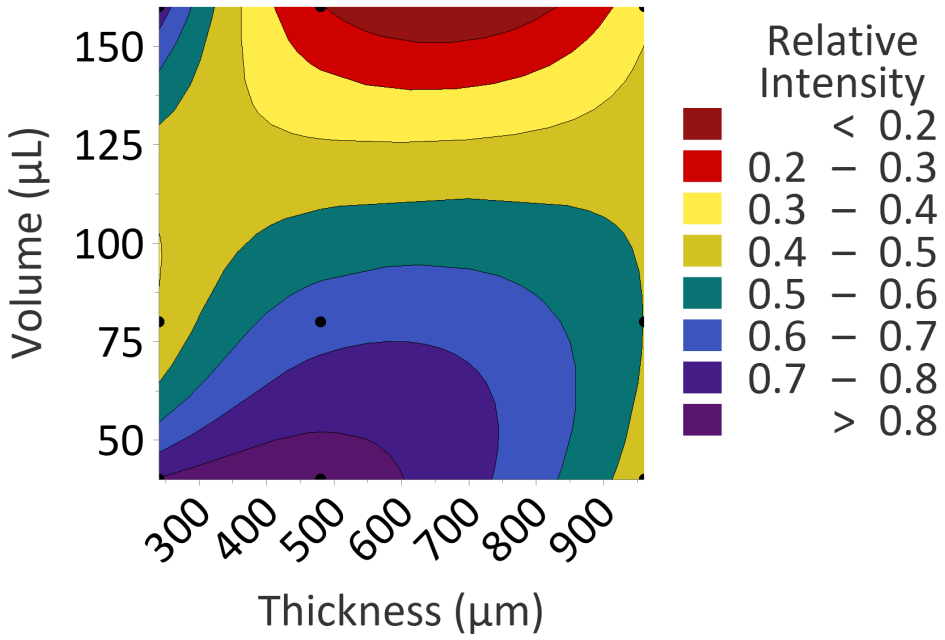

Figure 2. Contour plot showing the change in relative intensity of the CQD 520 nm-530 nm emission peaks.

There is a relation between the volume of CQDs dispersed, the thickness of the 3D printed structure, and physical interactions between the CQDs and the SU-8-5 polymer. A thick structure would have a lower PL intensity than a thinner structure due to both the amount of reabsorption and the ability for the emitted photons to get out of the 3D printed structure. A higher volume of CQDs would increase the probability of reabsorption thereby lowering PL intensity, but Fig. 2 showed an increase in PL intensity when the structure was thin. This could be due to CT effects.

Next, this section goes over the PL lifetime decay when changing both the thickness of the 3D printed structure and the amount of CQDs loaded into the structure. The values used in the multicomponent exponential models in this paper can be seen in Appendix U. of Ref. [1]. From these values, the PL decay multicomponent exponential curve-fitted models for the experiment can be seen in Fig. 3.

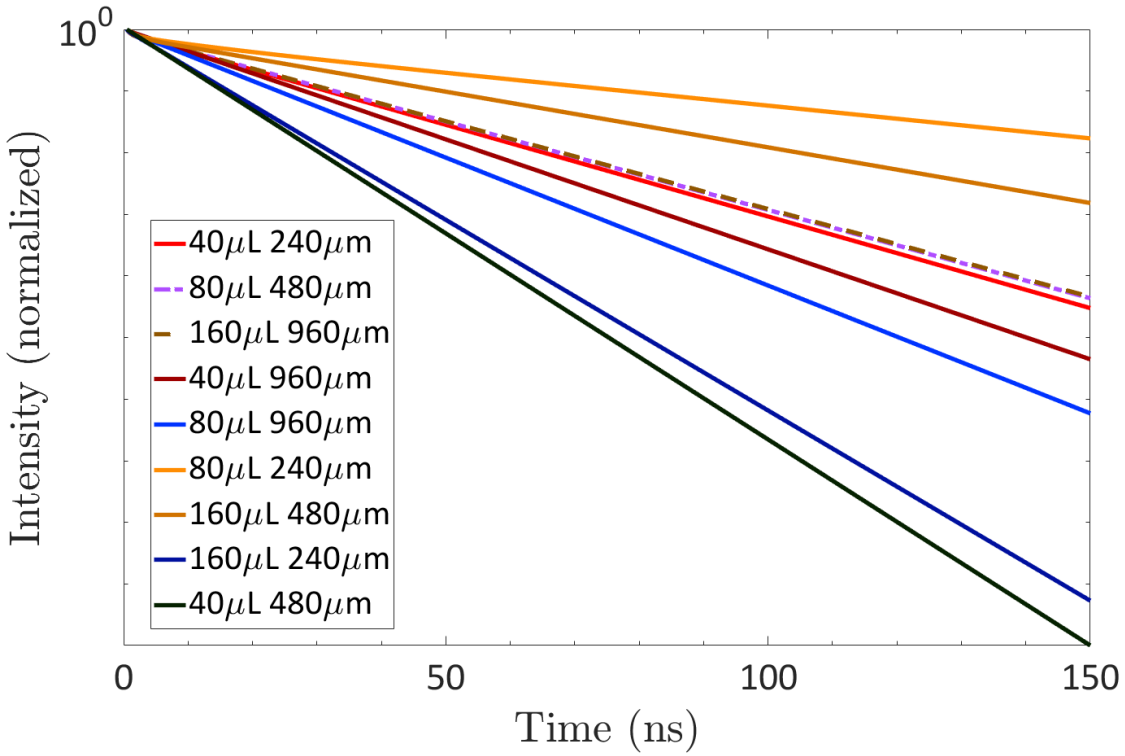

Figure 3. Multicomponent exponential model curve fitting of PL decay of CQDs applied as a 3D printed structure collected at CQDs' main peaks of emission.

It can be seen that all of the PL lifetime decays had variation. Minitab was used to create a PL lifetime decay contour plot. The decay time used was taken at 0.001% of the original amplitude. This contour plot can be seen in Fig. 4.

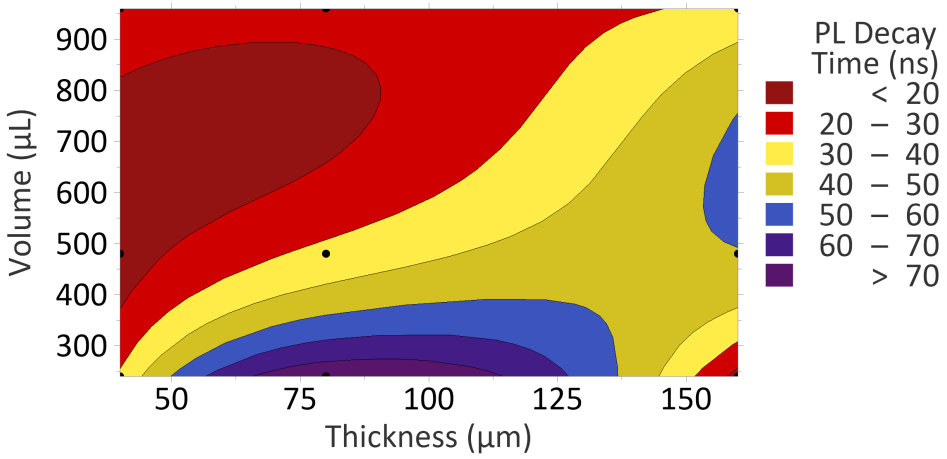

Figure 4. Contour plot showing the PL decay time at 0.001% of the original relative amplitude. This is measured off of the CQDs' emission peak of 520 nm-530 nm.

CT can be used to tune the PL lifetime decay of the materials investigated in this paper. Changing both the volume of CQDs dispersed into the 3D printed structure and the thickness of the 3D printed structure can allow one to optimize the PL lifetime decay for use in fast optical sensors.

5.0 CONCLUSIONS

This paper shows how one can tune both the relative PL emission of the CT emission peak and the PL lifetime decay at the CQDs' main peaks of emission. This can be done by using a unique fabrication technique of dispersing CQDs within a 3D printed honeycomb structure. The CT was determined to come from the SU-8-5 polymer used to cap the structure. The tunable CT has an effect on both the relative PL intensity and the PL lifetime decay, which has significance in terms of creating new sensors. Useful implications from this paper include: CQD emission can up-converted when in the proximity of a polymer designed to transfer their charge. This up-converting property could be useful for defense sensors and technologies such as NVGs. In addition, CQDs being used as fast x-ray scintillators would encourage future work into utilizing CT effects in tandem with organic scintillating polymers in this type of 3D printed structure [16–19]. Aside from CT effects, this paper encourages future work when wanting to use CQDs in radiation detection applications since the 3D printed structures can be used to stack CQDs. This stacking of CQDs in turn would increase the overall QE of the scintillating system. Since the 3D printed structure is made up of low-Z organic materials, this concept may also have use in neutron detection.

ACKNOWLEDGMENTS

This material is declared a work of the U.S. Government and is not subject to copyright protection in the United States. This research was supported in part by the U.S. Dept. of Energy, National Nuclear Security Administration under grant NA000103. This work was supported by the National Nuclear Security Administration of the U.S. Department of Energy under contract 89233218CNA000001. Approved for unlimited release, LA-UR-21-32338. Part of this work was performed at the Center for High Technology Materials, University of New Mexico, under the support of the Office of Naval Research Grants N00014-17-1-2975 and N00014-19-1-2117, and of the Navy HBCU/MI Program Grant N00014-18-1-2739. This work was performed, in part, at the Center for Integrated Nanotechnologies, an Office of Science User Facility operated for the U.S. Department of Energy (DOE) Office of Science. Los Alamos National Laboratory, an affirmative action equal opportunity employer, is managed by Triad National Security, LLC for the U.S. Department of Energy's NNSA, under contract 89233218CNA000001. The views expressed are those of the authors and do not reflect the official policy or position of the U.S. Air Force, Department of Defense, Department of Energy, the U.S. government, or the University of New Mexico.

6.0 REFERENCES

[1] M. Sherburne, "X-ray detection and strain sensing applications of colloidal quantum dots," Master's thesis, Air Force Institute of Technology, Mar. 2020.

[2] Y. Zhou, K. Mintz, C. Oztan, S. Hettiarachchi, Z. Peng, E. Seven, P. Liyanage, S. D. L. Torre, E. Celik, and R. Leblanc, "Embedding carbon dots in superabsorbent polymers for additive manufacturing," *Polymers*, vol. 10, no. 8, p. 921, Aug. 2018.

[3] L. Du, Z. Liu, and S. Jiang, "Inkjet-printed CdTe quantum dots-polyurethane acrylate thin films," *Journal of Nanomaterials*, vol. 2017, pp. 1–5, 2017.

[4] E. O. Chukwuocha, M. C. Onyeaju, and T. S. T. Harry, "Theoretical studies on the effect of confinement on quantum dots using the brus equation," *World Journal of Condensed Matter Physics*, vol. 02, no. 02, pp. 96–100, 2012.

[5] J. T. W. T. Jie Zhou, Yun Liu, "Surface ligands engineering of semiconductor quantum dots for chemosensory and biological applications," *Materials Today*, vol. 20, no. 7, Sep. 2017.

[6] G. Schmid, *Nanoparticles : from theory to application*. Weinheim: Wiley-VCH, 2004, ch. 3, pp. 93–95.

[7] X. Li, L. Gu, F. Zong, J. Zhang, and Q. Yang, "Temporal resolution limit estimation of x-ray streak cameras using a CsI photocathode," *Journal of Applied Physics*, vol. 118, no. 8, 2015.

[8] M. D. Sherburne, C. R. Roberts, J. S. Brewer, T. E. Weber, T. V. Laurvick, and H. Chandrahalim, "Comprehensive optical strain sensing through the use of colloidal quantum dots," *ACS Applied Materials & Interfaces*, vol. 12, no. 39, pp. 44 156–44 162, Sep. 2020.

[9] F. T. Rabouw and C. de Mello Donega, "Excited-state dynamics in colloidal semiconductor nanocrystals," *Topics in Current Chemistry*, vol. 374, no. 5, Aug. 2016.

[10] P. Kathirgamanathan, L. M. Bushby, M. Kumaraverl, S. Ravichandran, and S. Surendrakumar, "Electroluminescent organic and quantum dot LEDs: The state of the art," *Journal of Display Technology*, vol. 11, no. 5, pp. 480–493, May 2015.

[11] J. Alvelid, "Investigation of the photophysical properties of quantum dots for super-resolution imaging," Master's thesis, KTH Royal Institute of Technology, 2016.

[12] N. I. Hammer, T. Emrick, and M. D. Barnes, "Quantum dots coordinated with conjugated organic ligands: new nanomaterials with novel photophysics," *Nanoscale Research Letters*, vol. 2, no. 6, pp. 282–290, Jun. 2007.

[13] M. A. Rivera, "Metal to ligand and ligand to metal charge transfer bands," Online, Sep. 2019.

[14] J.-S. Chen, M. Li, and M. Cotlet, "Nanoscale photoinduced charge transfer with individual quantum dots: Tunability through synthesis, interface design, and interaction with charge traps," *ACS Omega*, vol. 4, no. 5, pp. 9102–9112, 2019. [Online]. Available: https://doi.org/10.1021/acsomega.9b00803

[15] F. Schaufele, I. Demarco, and R. N. Day, "FRET imaging in the wide-field microscope," in *Molecular Imaging*. Elsevier, 2005, pp. 72–94.

[16] A. Wieczorek, "Development of novel plastic scintillators based on polyvinyltoluene for the hybrid J-PET/MR tomograph," Ph.D. dissertation, Jagiellonian University, 2017.

[17] K. D. Rakes, "Evaluating the response of polyvinyl toluene scintillators used in portal detectors," Master's thesis, Air Force Institute of Technology, Mar. 2008.

[18] A. Tam, O. Boyraz, and M. Nilsson, "Plastic scintillator enhancement through quantum dot," *Hard X-Ray, Gamma-Ray, and Neutron Detector Physics XIX*, Aug. 2017.

[19] J. Park, H. Kim, Y. Hwang, D. Kim, and H. Park, "Scintillation properties of quantum-dot doped styrene based plastic scintillators," *Journal of Luminescence*, vol. 146, pp. 157–161, Feb. 2014.

7.0 LIST OF SYMBOLS, ABBREVIATIONS, AND ACRONYMS

CINT	Center for Integrated Nanotechnologies
COTS	Commercially-Off-The-Shelf
CQD	Colloidal Quantum Dot
CT	Charge Transfer
DoE	Design of Experiments
FRET	Förster Resonance Energy Transfer
FWHM	Full Width at Half Maximum
HOMO	Highest Occupied Molecular Orbital
IPA	Isopropyl Alcohol
IRF	Instrument Response Function
LUMO	Lowest Unoccupied Molecular Orbital
NVG	Night Vision Goggles
PCF	Photonic Crystal Fiber
PL	Photoluminescence
QE	Quantum Efficiency
SNL	Sandia National Laboratory
UV	Ultra Violet